

Shape Description of General, Curved Surfaces Using Tactile Sensing and Surface Normal Information

M. Charlebois, K. Gupta*, and S. Payandeh*

Experimental Robotics Lab (ERL), Simon Fraser University
School of Engineering Science, Burnaby, B.C. V5A 1S6, Canada

Abstract

In this paper we propose an approach for investigating the shape properties of objects with curved surfaces using tactile sensing by a dexterous robot hand. Our proposed Exploratory Procedure (EP) uses multiple fingers to slide along a surface while sensing contact points and surface normals. Our approach incorporates the surface normal information into a B-spline surface fit of the data gathered from this EP. This additional surface normal information was found to improve the approximation of the surface. The shape properties of this B-spline surface are analyzed to recognize the shape of the object. A confidence estimate of the estimated shape is also calculated.

1 Introduction

Humans rely heavily on their sense of touch when manipulating objects and gauging depth. Operators have discovered many problems controlling robotic manipulations using only a sense of vision. They have difficulty gauging depth without multiple camera angles which are not always available. Another problem is that small objects are occluded by the manipulator during manipulation tasks which makes it difficult to find the desired features of the object to grasp, or to orient the object.

Vision systems are also not practical in some hazardous environments. Using tactile sensing, a robot could orient itself by finding specific objects in the room. Some of these objects may be composed of curved surfaces and a method for recognizing them is required.

In order to examine the extent to which tactile sensing alone can be used to describe an object, a “Blind Man’s” approach is adopted in which tactile information from the tips of the fingers is the only sensing modality. This enables us to sense the contact point, and estimate the surface normal since the geometry of the fingertip and the configuration parameters of the manipulator are known.

Humans use specialized Exploratory Procedures (EPs) to extract specific information about an object as described by Klatzky and Lederman [10]. Their investigations also found that shape was the most highly diagnostic property for recognition. They describe a Contour Following EP

which humans use to determine the exact and local shape properties of an object.

We investigate an EP for shape perception using fingertip tactile sensors based on gliding on the surface of the unknown object. This EP was described previously in [3] as EP2 and will hereafter be referred to as EP2. Hemami, Bay, and Goddard proposed a similar EP in [8], however their focus was on the sensory requirements for performing the EP. Our methodology for obtaining shape information has been motivated by research in computer vision: [5], [6], [9], [12], and [13], who have investigated aspects of shape description and modelling based on curvature properties.

Tactile data is generally sparse and noisy. The data obtained from multiple fingers tracking a surface can be fit by a B-spline surface which acts like a low pass filter of the data. In our approach, the contact normal information is incorporated in the surface fitting procedure to assist in the approximation of the shape of the surface. A weighing matrix enables the surface fit to preferentially approximate the tangents or position data at each point. *The primary motivation for incorporating the surface normal information is to provide additional constraints for the surface fit in the finger-to-finger direction.*

2 Overview

We propose a method to investigate the shape properties of an object using EP2. We assume that a dexterous robot hand with semi-spherical fingertip tactile sensors is used to probe an object. Shape properties for a surface patch can be analyzed from data collected by sweeping multiple fingers of the dexterous hand across a surface.

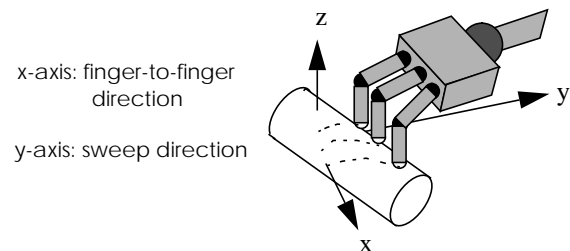


Fig. 1. Three fingers tracking a rotated cylinder (EP2)

* These authors are listed in alphabetical order

Research has been supported by NSERC grants for Drs. Gupta and Payandeh

Figure 1 shows EP2 being performed on a cylinder rotated about the z-axis. The x and y axes are determined from the finger-to-finger, and sweep directions respectively.

The overall algorithm for analyzing a surface using EP2 is as follows:

1. Track the surface using three fingers of a dexterous hand and record the information required to determine the contact positions and surface normals.
2. Transform the data to a desired coordinate frame and scale for performing the surface fit.
3. Fit a B-spline surface to the data points using the surface normal information using either a tangent or position weighed fit.
4. Calculate the shape parameters on a discretized grid over the B-spline surface and calculate the mean and standard deviations of these parameters
5. Determine the best approximating shape based on the mean and standard deviation of the shape parameters.

The shape properties at a point are curvature based and are invariant to scale and orientation. Shape properties will be determined from the estimated principal curvatures over the patch. The information gathered about the shape of the object can be used to orient the patch, guide further exploratory actions, or be used toward shape description or object recognition.

Shape analysis is performed using shape parameters (S, R) defined by Koenderink [9] instead of HK sign maps as in [13]. The S parameter provides a qualitative estimate of the object's shape and the R parameter gives a quantitative estimate of its curvedness which is related to its size. We can calculate a confidence estimate of the shape parameter values over a grid on the B-spline surface.

There has not been much research into shape description of curved surfaces from tactile sensing. Allen and Michelman [1] have investigated the usage of EPs to recognize surfaces of revolution from their contours. In this research, we are investigating a way to analyze more general curved surfaces and extract higher level shape information. Fearing [7] has also investigated recovering shape from extremely sparse tactile data. He attempted to recover a much restricted class of shape models from convex Linear Straight Homogeneous Generalized Cylinders (LSHGC) from three finger contacts. Using the position, surface normal, and curvature information at the contacts, Fearing attempted to solve the constraint equations of the LSHGC with limited success.

The structure of the paper is as follows. Section 3 provides background information. Section 4 describes how the surface normal information is integrated into the surface fitting algorithm. The simulation results are presented in

section 5 and the results of the actual experiments are shown in section 6. A discussion of EP2 and the conclusions of our experiments are presented in section 7.

3 Background

This section provides a brief overview of B-spline curves, the calculation of curvature at a point, and qualitative shape measures.

3.1 B-spline Curves and Surfaces

Detailed descriptions of B-splines, B-spline surfaces and surface fitting can be found in [4] and [11].

The equation for an k th order B-spline with n basis functions is shown in equation 1. For a p segment spline, the number of basis functions is $k+p-1$.

$$S(x) = \sum_{i=1}^{n+1} c_i N_{i,k}(x) \quad S(x) \Rightarrow (x, y) \quad (1)$$

where $N_{i,k}(x)$ are the values of the B-spline basis functions at x for the current set of knot vectors, and c_i are the *control points* which define the curve. The curve may be translated or rotated by transforming the control points. This is one of the primary benefits of the B-spline representation of a surface.

The x parameter is defined on the interval $[x_{min}, x_{max}]$. The spline is only defined in this interval. If a single, k th order spline segment was used, the knot vector would be composed of k values of x_{min} followed by k values of x_{max} . The spacing and number of the knots in the knot vector determine the basis functions over the interval.

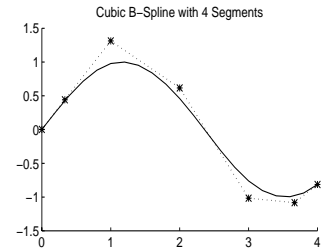


Fig. 2. Cubic B-spline curve and control points

Figure 2 shows a cubic B-spline with 7 control points, and uniform knot spacing. The knot vector for the curve is $[0 \ 0 \ 0 \ 0 \ 1 \ 2 \ 3 \ 4 \ 4 \ 4 \ 4]$.

The linear system of equations for the B-spline curve is:

$$EC = Y$$

$$E = \begin{bmatrix} N_{1,k}(x_1) & \dots & N_{n+1,k}(x_1) \\ \dots & \dots & \dots \\ N_{1,k}(x_g) & \dots & N_{n+1,k}(x_g) \end{bmatrix} \quad C = \begin{bmatrix} c_{1x} & c_{1y} \\ \dots & \dots \\ c_{nx} & c_{ny} \end{bmatrix} \quad (2)$$

where E is the *observation matrix* for the vector of x values of the data points, C is the matrix of control points, and Y is the matrix of x and y values of the B-spline for the corresponding x values used in the E matrix.

The standard least squares formulation problem for g data points (x_r, y_r) , requires minimization of the error (δ) according to the following equation:

$$\delta = \sum_{r=1}^g (w_r y_r - w_r S(x_r))^2 \quad (3)$$

where w_r is the weighing factor for the r th data point.

The weighted least squares solution of the control points can then be obtained by:

$$C = \left(E^T W E \right)^{-1} E^T W Y \quad (4)$$

where W is the matrix of weighting factors.

This formulation can be extended for bivariate B-spline surfaces. The equation for an k th order bivariate B-spline with n basis functions in x and m basis functions in y is:

$$S(x, y) = \sum_{i=1}^{n+1} \sum_{j=1}^{m+1} c_{i,j} N_{i,k}(x) M_{j,k}(y) \quad (5)$$

The basis function in x and y are denoted by $N_{i,k}(x)$ and $M_{j,k}(y)$ respectively. The basis splines in the x direction are dependant only on the x coordinate of the data points, likewise for the basis splines for the y direction. Therefore, the observation matrix for one bivariate patch can be written as the Kronecker product of the basis function in x and y :

$$E = N \otimes M \quad (6)$$

where

$$N = \begin{bmatrix} N_{1,k}(x_1) & \dots & N_{n+1,k}(x_1) \\ \dots & & \dots \\ N_{1,k}(x_g) & \dots & N_{n+1,k}(x_g) \end{bmatrix} \quad (7)$$

$$M = \begin{bmatrix} M_{1,l}(y_1) & \dots & M_{m+1,l}(y_1) \\ \dots & & \dots \\ M_{1,l}(y_g) & \dots & M_{m+1,l}(y_g) \end{bmatrix}$$

The least squares fit for the surface can be solved by:

$$C = \left(E^T W E \right)^{-1} E^T W Z \quad (8)$$

where the Z matrix contains the x , y and z coordinates of the sample points. The C matrix is the matrix of control points which define the B-spline surface.

3.2 Gaussian, Mean, and Principal Curvatures

The curvature at a point on a surface is characterized by its principle curvatures ($Kmin$ and $Kmax$). The Gaussian curvature is the product of the principal curvatures. The mean curvature is the average of the principal curvatures. A more complete description can be found in [5], and [6]. Consider a surface $Q(u, v)$.

Define the variables E, F, G , and e, f, g as:

$$E = \frac{\partial Q}{\partial u} \cdot \frac{\partial Q}{\partial u} \quad F = \frac{\partial Q}{\partial u} \cdot \frac{\partial Q}{\partial v} \quad G = \frac{\partial Q}{\partial v} \cdot \frac{\partial Q}{\partial v} \quad (9)$$

$$e = \frac{\partial^2 Q}{\partial u^2} \cdot \bar{n} \quad f = \frac{\partial^2 Q}{\partial u \partial v} \cdot \bar{n} \quad g = \frac{\partial^2 Q}{\partial v^2} \cdot \bar{n}$$

where \bar{n} is the unit surface normal. The Gaussian and mean curvature are then respectively:

$$Kg = \frac{(eg - f^2)}{(EG - F^2)} \quad Ka = \frac{(Eg - 2Ff + Ge)}{2(EG - F^2)} \quad (10)$$

The minimum and maximum curvatures can be determined from the Gaussian and mean curvatures by:

$$Kmax = Ka + \sqrt{Ka^2 - Kg} \quad (11)$$

$$Kmin = Ka - \sqrt{Ka^2 - Kg}$$

3.3 Qualitative Shape Measures

Regardless of the size of a sphere, all spheres have the same shape. ‘‘Shape’’ is a quality, ‘‘size’’ is the quantity. Koenderink [14]* proposes a representation of shape using two parameters: R and S . The definitions of these parameters are as follows.

$$R = \sqrt{\frac{(Kmin^2 + Kmax^2)}{2}} \quad (12)$$

$$S = -\frac{2}{\pi} \text{atan} \left(\frac{Kmax + Kmin}{Kmax - Kmin} \right)$$

The R parameter is quantitative in nature and represents the curvedness of the patch. R ranges from zero for flat surfaces to infinity at a perfectly sharp edge. The S parameter is qualitative in nature and represents the shape of the patch. Figure 3 shows how the S parameter maps shapes into the interval $[1, 1]$.

Using this mapping, it is possible to calculate the mean and standard deviation of the values of S and R for a grid of points on a surface. The standard deviations of S and R can be used as a confidence measure of their values.

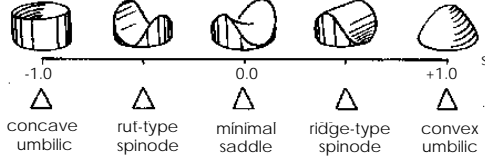


Fig. 3. Koenderink's shape parameter [9]

4 Using Surface Normal Information

When only the contact information from three fingers is used we are limited to a quadratic fit of the data in the finger-to-finger direction. Any position error in the measurements of the contact positions will be fit. Using the tangent information, six equations are available for solving for the B-spline in the finger-to-finger direction. The tangent information requires that the least squares fit is also a least squares fit for the derivative information as well. This is important when performing a curvature based shape analysis.

4.1 Converting Surface Normals to Tangents

We formulate the surface fitting problem such that the derivatives of a B-spline use the same B-spline coefficients as the original spline. Using this approach the tangent information is easily incorporated into the least squares solution.

First the surface normals are converted into derivatives in the x and y directions using the following equations.

$$\frac{\partial}{\partial x} P(x, y) = \frac{-n_x}{n_z} \quad \frac{\partial}{\partial y} P(x, y) = \frac{-n_y}{n_z} \quad (13)$$

$$\bar{n} = [n_x \ n_y \ n_z]^T$$

4.2 Surface fitting Using Tangents

The least squares surface fitting problem including the tangent information is then that of minimizing the augmented equation for g data points:

$$\delta = \sum_{r=1}^g \left(\left(w_{1r} z_r - w_{1r} S(x_r, y_r) \right)^2 + \left(w_{2r} t_{x_r} - w_{2r} S_x(x_r, y_r) \right)^2 + \left(w_{3r} t_{y_r} - w_{3r} S_y(x_r, y_r) \right)^2 \right) \quad (14)$$

where t_x and t_y are the tangents in x and y , and w_1 , w_2 , and w_3 are the weights for the data points, tangents in x , and tangents in y respectively.

The tangents in the x and y directions can be obtained from the surface normals at the contacts. The observation matrices of basis functions in x and y are denoted by N and M

respectively. Observation matrices for the derivatives of the basis splines in x and y are denoted by N' and M' and are easily calculated. The composition of the observation matrix for the single bivariate patch including the tangent information is:

$$\begin{aligned} E1 &= N \otimes M \\ E2 &= N' \otimes M \\ E3 &= N \otimes M' \end{aligned} \quad E = \begin{bmatrix} E1 \\ E2 \\ E3 \end{bmatrix} \quad (15)$$

The least squares fit for the surface can be solved by:

$$C = \left(E^T W E \right)^{-1} E^T W Z \quad (16)$$

where the Z matrix contains the x , y and z coordinates of the sample points. The C matrix is the matrix of control points which define the B-spline surface. The weighing matrix W , enables the surface fit to preferentially approximate the position or the tangent at each point.

5 Simulation Studies

EP2 was performed in simulation on cylindrical, spherical and planar objects. The mean and standard deviation of Koenderink's shape parameters (S , R) were calculated over a 4×4 grid in the surface. A small grid was used to minimize computation time. The shape of the sensed patch could be determined by comparing its S , and R parameters to the known values for the objects. This method assumes that the shape parameter value for the sensed region of the object is constant.

Simulations were performed to investigate the effect of the order of the fit and the radius of the cylinder, or sphere on the accuracy of the estimate of S . The range of radii used in the experiments was between 5.7 and 1000 units. Simulations were also performed to analyze the effect of rotating the object on the accuracy of the shape analysis.

5.1 Cylinder

Simulations were performed to analyze the effect of rotating the cylinder on the accuracy of the shape analysis. Rotations of 0, 10, 30, 45, 60, 80, and 90 degrees were used and cylinders of radius 6, 10 and 20 were simulated. The root mean squared (RMS) error of the estimation of S for each rotation of each cylinder is shown in figure 4.

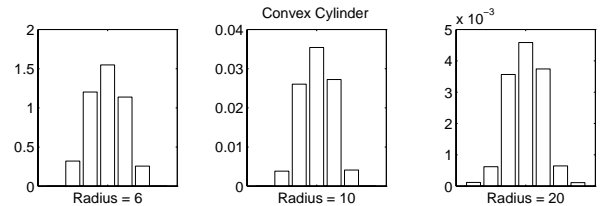


Fig. 4. RMS error in S for rotations of 3 cylinders

The error in the estimation of S is highest for a rotation of 45 degrees and minimal for rotations of 0 and 90 degrees. In the latter case, the B-spline parameter directions are aligned with the principal direction of curvature. In the former case the B-spline parameter directions are at 45 degrees to the principal directions of curvature of the cylinder.

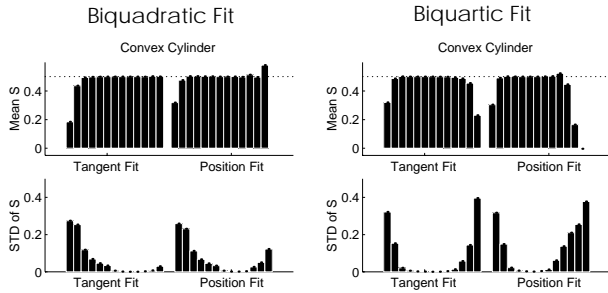


Fig. 5. S values and standard deviations of S for cylinders of various radii

In order to obtain the worst case fit, the cylinders were rotated 45 degrees for the next experiment, based on the results of the previous simulation. EP2 simulations were performed for cylinders with radii between 5.7 and 1000 units. Figure 5 shows the results of the estimated values of S . The first group show the estimated values of S for tangent weighted fits, the second are for the position weighted fits. The results for the biquadratic and biquartic surface fits are shown. The expected value of S for a convex cylinder is 0.5 and is indicated by the dotted line.

Accurate estimates of S were obtained for radii between 6 and 300 units. The tangent weighed fit was more accurate and had a smaller standard deviation for the large radii than the position weighed fit. This is likely a result of analyzing such a coarse grid of the surface.

5.2 Sphere

Simulations were also performed for the spheres of the same radii, for tangent and position weighed fits, and for biquadratic, bicubic, and biquartic B-spline surface fits. The expected value of S for a sphere is 1.0. The results for the biquadratic and biquartic surface fits are shown in figure 6.

As the order of the bivariate B-spline increases, the accuracy of the estimate of S decreases for spheres with a large radius. The tangent weighed fit is more accurate than the position weighed fit for spheres with a large radius.

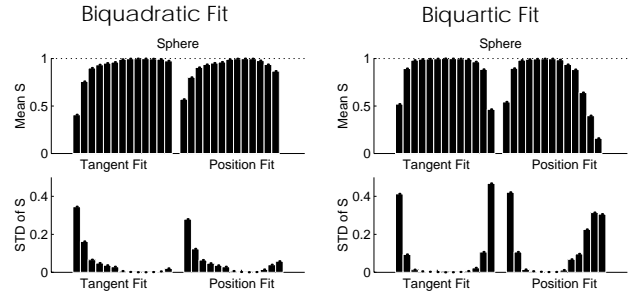


Fig. 6. S values and standard deviations of S for spheres of various radii

This surface fitting approach could not successfully classify the sphere of radius 5.7, using either position or tangent fitting and a bivariate surface of order 5 (quartic) or less. The best estimates of S for spheres of large radius were obtained with a biquadratic surface fit.

5.3 Planes

Three different plane equations were tracked using EP2. The mean and variance of R over the patch was analyzed, and all of the planes were successfully classified. The standard deviation of R was negligible.

5.4 Summary of Simulation Results

Several simulations were performed to analyze the feasibility of using EP2 to obtain information about the shape of a surface and to recognize simple shape primitives.

The accuracy of the estimate of S was affected by:

- The order of the approximation surface
- The angle between the directions of principal curvature of the surface and the x and y directions of the B-spline surface (maximum at 45 degrees)
- The radius of curvature of the object
- Whether the approximating surface was tangent weighted or position weighted

Accurate estimates of S can be obtained for spheres, and convex and concave cylinders over a range of radii. Planar surfaces can also be easily recognized.

The standard deviation of S was quite high when the estimate of S was incorrect and was a good indication that the estimate was incorrect.

6 Experiments

Experiments were performed to test the effect of sensor noise on our approach for investigating shape. In order to obtain the data for three fingers of a dexterous robot hand performing EP2, a single probe made three passes of each surface. The probe has a circular end to simplify the calculation of the contact position and surface normal, and is

mounted on a force/moment sensor. This sensor is attached to the 3 DOF robot as shown in figure 7. A discrete sampling of the surface was performed by the robot instead of tracking across the surface in order to simplify the control aspects of EP2.

Six points along the surface were probed with each finger. At each point, two data samples were taken to verify the integrity of the data. Therefore, a total of 36 data points were acquired for each surface. The joint angles of the robot and the x and y forces measured at the force sensor are taken for each data point. A sample is taken when the force sensor exceeds a desired threshold.

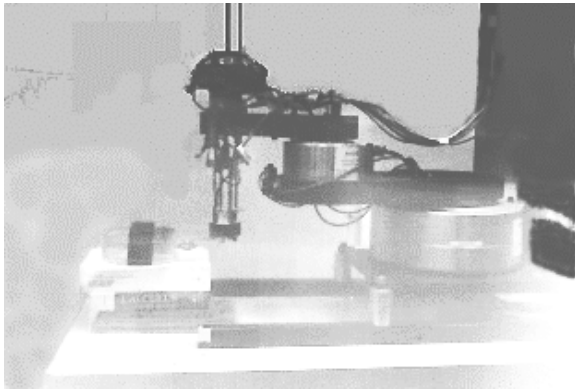


Fig. 7. Freddy performing EP2 experiment

An 8×8 grid of points on the surface was analyzed to determine the mean values of S and R and their standard deviations.

6.1 Planar Surface

Figure 8 shows the biquadratic surface fit of the data and the control points of the surface.

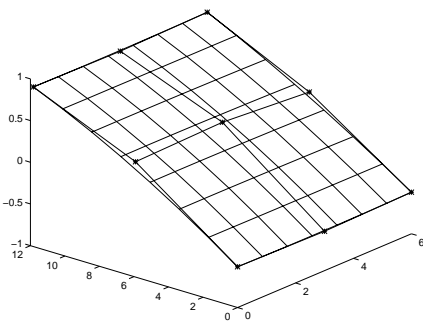


Fig. 8. Biquadratic fit of planar surface with its control point mesh shown

The results of the calculation of the mean and standard deviation of S and R for biquadratic, position and tangent weighed fits are shown in table 1. The expected value of R for a plane is zero. The mean value of R calculated from

the surface was found to be very small, although significantly higher than for the simulation data. However, the standard deviation (S.D.) of R was very small which means that the surface is uniform in its curvedness. The standard deviation of the S parameter is fairly high because the principal curvatures are nearly zero. If the R parameter were exactly zero (i.e. the principal curvatures were exactly zero) the S parameter would be undefined.

Table 1: Results of Shape Analysis of Planar Surface

Fit	S	S.D. of S	R	S.D. of R
Tangent	0.4703	0.21204	0.004114	0.0006562
Position	0.3643	0.24721	0.003026	0.0009828

It was found that, the noise in the data is best suppressed by a biquadratic fit. The position weighed fits had a similar error in the approximation of S . The approximations of S using higher order surfaces were much less accurate and had higher standard deviations.

6.2 Convex Cylindrical Surface

A convex cylindrical surface of radius 6.6 cm was placed in the workspace to be probed. The data was gathered as it was for the planar surface.

Figure 9 shows the surface fit of the data and the control points of the surface.

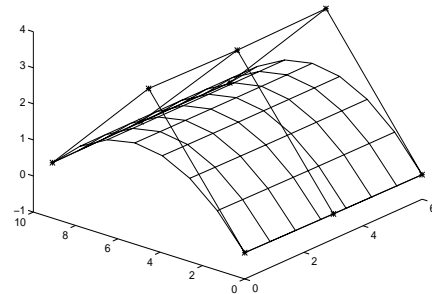


Fig. 9. Biquadratic fit of convex cylindrical surface with its control point mesh shown

The results of the mean and standard deviation of S and R , and estimated radius are shown in table 2.

Table 2: Results of the Shape Analysis of the Convex Cylindrical Surface

Fit	S	S.D. of S	R	S.D. of R	Radius
Tangent	0.4980	0.009639	0.080290	0.024210	8.8078
Position	0.5014	0.015773	0.073446	0.016892	9.6304

The expected value of R for a cylinder of radius 6.6 is 0.1071. The mean value of R calculated from the surface was close to this value. The standard deviation of R was between 22 and 30 percent of the estimated value.

The expected value of S is 0.5 which is very close to the values estimated for the surface for both the tangent and position weighed fits. The S parameter of the tangent weighed fit has a standard deviation slightly smaller than for the position weighed fit.

The estimated radius of the cylinder is more accurate for the tangent weighed fit. The accuracy of the quantitative characteristics of the surface is fairly low. The radius was measured within an accuracy of 1/3 of the actual radius.

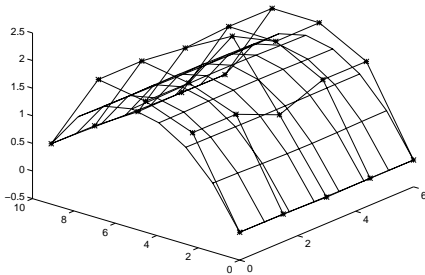


Fig. 10. Biquartic fit of convex cylindrical surface with its control point mesh shown

The bicubic, tangent weighed fit was nearly planar on one side. The biquartic tangent weighed fit shown in figure 10, had a similar shape to the bicubic fit, although slightly more noisy.

7 Discussion and Conclusions

We presented an approach using a multi-finger contour following EP to determine the shape properties of an approximating surface based on its principal curvatures. The surface patch was approximated by a B-spline surface which incorporated the contact normal information.

The proposed method for acquiring data using EP2 has been verified experimentally using a manipulator equipped with a force/moment sensor to detect the contact position and surface normal. The method was capable of acquiring sufficiently accurate data to enable the estimation of the shape parameters of the surface.

The S parameter for the convex and concave cylinders could be estimated within 0.012 units of the actual value and with a standard deviation of less than 0.04 units for the concave cylinder. Even with coarse sensor resolution, we were able to obtain good results for qualitative shape recognition.

The accuracy of the shape estimation was found to depend on the alignment of the principal curvatures with the coordinate system of the B-spline. A second iteration of EP2 could be performed with the sweep directions aligned with one of the principal directions of curvature. This approach would provide the greatest accuracy for estimating the shape of the surface.

If the object being sensed is a single primitive then the shape can be recognized from a small patch. If the object is composed of a combination of shape primitives, the individual primitives can first be recognized and then the object can be determined from the adjacency graphs of the primitives for instance.

8 References

- [1] P. K. Allen and P. Michelman, "Acquisition and Interpretation of 3-D Sensor Data from Touch", *IEEE T. on Robotics and Automation*, Vol. 6, No. 4, pp. 397-404, 1987
- [2] R. C. Beach, "An Introduction to the Curves and Surfaces of Computer Aided Design", Van Nostrand Reinhold, New York, 1991
- [3] M. Charlebois, K. Gupta, and S. Payandeh, "Curvature Based Shape Description Using Tactile Sensing", *IEEE ICRA*, Vol X, pp. 3502-3507, 1996
- [4] P. Dierckx, "Curve and Surface Fitting with Splines", Clarendon Press, New York, 1993
- [5] J. C. Dill, "An application of Color Graphics to the Display of Surface Curvature", *Computer Graphics*, Vol. 15, No. 3, August 1981
- [6] G. Elber and E. Cohen, "Second-Order Surface Analysis Using Hybrid Symbolic and Numeric Operators", *ACM Transactions on Graphics*, Vol. 12, No. 2, pp. 160-178, April 1993
- [7] R. S. Fearing, "Tactile Sensing for Shape Interpretation", *Dexterous Robot Hands*, S. T. Venkataraman and T. Iberall, Springer-Verlag, 1990
- [8] H. Hemami, J. Bay, and R. E. Goddard, "A Conceptual Framework for Tactually Guided Exploration and Shape Perception", *IEEE Transactions on Biomed. Eng.*, Vol. 35, No. 2, pp. 99-109, Feb 1988
- [9] J. J. Koenderink, "Solid Shape", The MIT Press, Cambridge, M.A., 1990
- [10] S. J. Lederman, R. L. Klatzky and D. T. Pawluk, "Lessons From the Study of Biological Touch for Robotic Haptic Sensing", *Advanced Tactile Sensing for Robotics*, H. R. Nicholls, World Scientific, 1992
- [11] D.F. Rogers and J. A. Adams, "Mathematical Elements for Computer Graphics", McGraw-Hill, New York, 1990
- [12] S. S. Sinha and P. J. Besl, "Principal Patches a Viewpoint Invariant Surface Description", *IEEE ICRA*, Vol. 1, pp. 226-231, 1990
- [13] E. Trucco and Robert B. Fisher, "Experiments in Curvature-Based Segmentation of Range Data", *IEEE PAMI*, Vol. 17, No. 2, pp. 177-182, Feb 1995